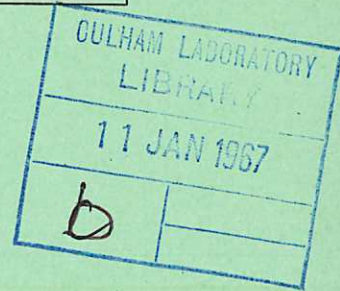


This document is intended for publication in a journal, and is made available on the understanding that extracts or references will not be published prior to publication of the original, without the consent of the authors.



United Kingdom Atomic Energy Authority

RESEARCH GROUP

Preprint

THE TRAPPING OF HYDROGEN IONS IN MOLYBDENUM TITANIUM TANTALUM AND ZIRCONIUM

G. M. McCracken

J. H. C. Maple

Culham Laboratory,
Culham, Abingdon, Berkshire

1966

Enquiries about copyright and reproduction should be addressed to the Librarian, UKAEA, Culham Laboratory, Abingdon, Berkshire, England

UNCLASSIFIED
(Approved for publication)

CLM - P 118

THE TRAPPING OF HYDROGEN IONS IN MOLYBDENUM,
TITANIUM, TANTALUM AND ZIRCONIUM

by

G.M. McCracken
J.H.C. Maple

UKAEA Research Group,
Culham Laboratory,
Nr. Abingdon,
Berks.

August, 1966 (P/H)

A B S T R A C T

The trapping of hydrogen ions in these metals has been measured by a mass spectrometric technique. Targets are bombarded by a mass analysed ion beam of 10- 100 μ A at 3-30 keV in a target chamber at $\sim 10^{-9}$ torr. The rise in partial pressure of hydrogen in the target chamber is measured during bombardment, and subsequently during thermal desorption. The absolute trapping coefficient can then be calculated from the ratio of the total quantities of hydrogen emitted during these two measurements.

The trapping coefficients have been measured as a function of dose and energy. It was found that Mo had initially a high trapping coefficient but that the trapping coefficient rapidly decreases with dose and saturation is reached at $\sim 10^{17}$ ions/cm² at room temperature. Ti, Ta and Zr exhibit markedly different behaviour. Trapping coefficients as high as 0.92 are observed and these are maintained constant with dose up to the maximum so far used of nearly 10^{19} ions/cm². No appreciable variation of the trapping coefficient with energy in the range investigated has been observed.

These results have been interpreted in terms of a model taking into account the diffusion coefficient of hydrogen in the metal and the potential barrier for hydrogen atoms at the surface.

C O N T E N T S

	<u>Page</u>
1. INTRODUCTION	1
2. APPARATUS	1
3. METHODS OF MEASURING TRAPPING COEFFICIENT η	2
4. RESULTS	5
4.1 Absolute Trapping Coefficients: Molybdenum	5
4.2 Absolute Trapping Coefficients: Ti, Ta, Zr.	6
4.3 Observations of Gas Sputtering	7
4.4 Dependence of η on dose	8
4.5 Energy Dependence of η	9
5. DISCUSSION	10
6. CONCLUSION	14
ACKNOWLEDGEMENTS	15
REFERENCES	16

1. INTRODUCTION

The trapping of energetic ions in metals has been studied extensively in recent years⁽¹⁻⁵⁾. It is of considerable practical importance in devices such as sputter ion pumps and in the preparation of samples in electromagnetic separators. In spite of this, however, the mechanism of the interaction of the ions with the solid lattice is not completely understood, and in particular the phenomenon known as gas sputtering which affects the saturation of the target is still the subject of discussion⁽⁶⁾.

In the investigations mentioned so far work has been primarily concentrated on the interaction of rare gas ions with metal surfaces in an attempt to elucidate the physical mechanisms without the complication of using ions which may also react chemically with the target material. Recently however the importance of trapping hydrogen ions has been recognised in large thermonuclear devices, and with hydrogen ions chemical reactions may well take place. There have been conflicting results as to the trapping coefficient of hydrogen ions in metals^(7,8), and the present work has been undertaken with the aim of trying to resolve the previous uncertainties.

Because of the wide range of energies with which the secondary particles may be re-emitted from the metal surface and the uncertainty as to their charge state, the simplest method of measuring the total number of re-emitted particles appeared to be to measure the change in pressure produced when a target is bombarded⁽⁸⁾, or to measure the number of ions buried by subsequent thermal desorption⁽³⁾. In the present study a combination of these two techniques has been used.

2. APPARATUS

The apparatus is shown schematically in fig. 1. It has been described in detail in an earlier publication⁽⁹⁾. The ion beam is extracted from an R.F. source, accelerated to an energy in the range 5-30 keV, mass analysed and focussed onto the target. Particular attention has been paid to the vacuum system which is constructed throughout of stainless steel with bakeable valves and gold wire gaskets.

There are four differential pumping stages between the source

and the target chamber. The main gas load from the source is taken by a mercury diffusion pump operating at 3,000 l/sec for hydrogen. In the following three stages sputter ion pumps are used to avoid the possibility of hydrocarbon contamination. Finally the target chamber is pumped by a titanium sublimation pump with a speed in excess of 10^4 litre/sec. The base pressure in the outer target chamber (see fig. 1) is normally $1-2 \times 10^{-10}$ torr and the pressure in the presence of a $20 \mu\text{A}$ beam is $\approx 4 \times 10^{-10}$ torr (N_2 equivalent). Maximum beam current is $300 \mu\text{A}$ over 0.1 cm^2 . The pressure in the inner target chamber does not normally rise above 5×10^{-9} torr (N_2 equivalent) with a $20 \mu\text{A}$ beam thus giving conditions under which the beam to background gas bombardment ratio is $\sim 10^2$.

A quadrupole mass filter with a nude ion source is mounted in the inner chamber (fig. 2). The targets are mounted on a turntable with six positions each of which can be brought in line with the beam in turn. The turntable is mounted on a molybdenum shaft rotating in boron nitride bearings and is rotated by a "wobble stick" welded into a stainless steel bellows as shown in fig. 2. The targets, normally $2 \times 1.25 \times 0.025 \text{ cm}$ are supported by split tubes on the end of 1 mm molybdenum rods. They may be heated by electron bombardment from behind up to $\sim 2000^\circ\text{K}$.

The ion beam after being mass analysed and refocussed by an electrostatic quadrupole lens pair, passes through the main target chamber and enters the inner target chamber where it strikes the target. The passage of the beam through the outer chamber where the pressure is $\sim 5 \times 10^{-10}$ torr before it enters the inner target chamber, avoids the possibility of neutral gas flow interfering with the pressure rise measurement. The beam is defined by a 5 mm dia. hole and electrons in the beam are suppressed just before entering the inner chamber. The target is held at a positive potential with respect to earth to suppress secondary electrons produced when the beam strikes the target.

3. METHODS OF MEASURING TRAPPING COEFFICIENT η

Earlier experiments using similar apparatus to measure trapping coefficients of hydrogen ions in stainless steel showed considerable disagreement. Work carried out by Simonov et al⁽⁷⁾ indicated that saturation (i.e. $\eta = 0$) was reached after bombarding stainless steel targets with doses $> 10^{17} \text{D}_1^+$ ions/ cm^2 at 20 keV.

Early work by Borovik⁽⁸⁾ however, indicated a trapping coefficient of 0.95 at 35 keV for hydrogen ions at doses up to at least 10^{19} ions/cm². More recent work by the present authors⁽¹⁰⁾ indicated a constant trapping coefficient of ~ 0.5 for doses $> 10^{17} < 10^{19}$ of H_1^+ ions in stainless steel, molybdenum and tungsten. This value was moreover constant within a few per cent over the energy range 5-30 keV, but there was an uncertainty in the absolute value, which could have amounted to a factor of 2. The reason for this uncertainty, and in our opinion the major objection to experiments of this type, is the difficulty of obtaining an absolute measurement of pressure. Accurate pressure measurements are particularly difficult to achieve with hydrogen in the ultra high vacuum region because of the chemical and physical interactions it has with the ion gauge. In another recent paper Borovik et al⁽¹¹⁾ have shown that this source of inaccuracy was to some extent responsible for their earlier high trapping coefficients and the remeasured value now appeared to be 0.5 for stainless steel at room temperature. This value seemed to be confirmed by another measurement made at the same time using a weighing technique.

In view of the confused situation we have undertaken these experiments again and have modified the original technique so that the absolute trapping coefficients can be measured from the ratio of two pressure measurements without any absolute pressure calibration. This is accomplished by combining the original measurements with the thermal desorption technique described by Kornelson⁽³⁾. The original method (to be called Method I) consisted in measuring the partial pressure rise in the vicinity of the target during ion bombardment. Assuming that no neutral gas is introduced with the beam and that the re-emitted particles thermalize without multiplication on the other surfaces of the chamber the trapping coefficient is given by

$$\eta = 1 - R = 1 - \frac{2eAS\Delta p \times 273}{22.4 \times 760 \times 293 \times I} \quad \text{at } 20^\circ\text{C}$$

$$= 1 - 10.6 \frac{\Delta p \cdot S}{I} \quad \dots (1)$$

where Δp is the rise in partial pressure of hydrogen in torr.

S is the pumping speed out of the chamber in l/sec.

A is Avogadro's number.

I is the ion beam current in amps.

e is the charge on the proton.

R is the re-emitted fraction of the beam.

If after the target is bombarded it is then heated, so that all the trapped hydrogen ions are released and the pressure rise during this release is measured with the same gauge under exactly the same conditions as in the first set of measurements, then the average trapping coefficient during the bombardment can be calculated from the ratio of the total quantity of gas released during the bombardment to the sum of the quantity of gas released during bombardment and that released during subsequent thermal desorption, i.e.

$$\eta = 1 - R = 1 - \frac{\int f(p_b) dt}{\int f(p_d) dt + \int f(p_b) dt} \quad \dots (2)$$

where $f(p_b)$ is the variation of pressure during bombardment and $f(p_d)$ is the variation of pressure during subsequent thermal desorption. If the mass spectrometer is linear with pressure and the respective currents measured with it during bombardment and desorption are i_b and i_d , then

$$\eta = 1 - \frac{\int f(ki_b) dt}{\int f(ki_d) dt + \int f(ki_b) dt} \quad \dots (3)$$

i.e. η is independent of mass spectrometer sensitivity k , pumping speed of the system S and ion beam current I .

This method (to be called Method II) is convincing only if it can be unequivocally demonstrated that all the buried hydrogen can be thermally desorbed again. Obviously for many metals with low diffusion coefficients for hydrogen it may not be possible to drive off all the trapped hydrogen at any temperature below the melting point of the target. However once an absolute measurement of η has been obtained by Method II for a refractory metal in which it can be demonstrated that all the hydrogen is thermally desorbed, subsequent measurements can be made relative to the first measurement using Method I. In the present work Method II has been applied to Mo, Ti, Ta and Zr independently and then it is shown that all the measurements agree well with the relative trapping coefficients measured using Method I.

4. RESULTS

4.1 Absolute Trapping Coefficients: Molybdenum

The technique for measurement of absolute trapping coefficient was applied to molybdenum and an example taken with $95 \mu\text{A}$ of H_1^+ ions at 30 keV is shown in fig. 3. Because of the power input from the beam the target reaches a temperature of $\sim 500^\circ\text{C}$ and the temperature rise causes the small peak of thermally desorbed hydrogen at the beginning of the run. The amount of trapped gas is represented by the difference between the thermal desorption following the bombardment and the thermal desorption of a previously cleaned target as shown in fig. 3. Despite the very large number of ions with which the target has been bombarded (equivalent to 0.1 torr-litres) the number thermally released as gas at temperatures up to 1800°K is very small and is certainly less than 0.1% of the incident flux. Using equation 2 this leads to $\eta < .001$. The trapping coefficient has been measured in a similar manner with lower current densities and lower temperatures down to $\sim 100^\circ\text{C}$ with the same result. In order to eliminate the background hydrogen evolved from other surfaces when the target is heated to desorb the trapped hydrogen, the experiment was repeated using deuterium ions to bombard the target and monitoring the mass 4 deuterium peak with the quadrupole mass filter. A typical result is shown in fig. 4. Because of the lower beam current the target is at a lower temperature during bombardment and the rise to equilibrium level, indicating an initial change in trapping coefficient, is slower than in fig. 3 for hydrogen. Thus at this lower target temperature more of the incident ions are trapped initially. The negligible background with deuterium allows the ions to be more readily detected when they are thermally desorbed again as shown in fig. 4, and it is seen that the deuterium desorbed corresponds almost exactly with that trapped during bombardment if the plausible assumption is made that the equilibrium level p_0 corresponds to target saturation or $\eta = 0$.

$$\text{i.e. } p_0^t - \int f(p_b)dt = \int f(p_d)dt \quad \dots (4)$$

This experiment was repeated while varying the total charge It over a factor of 10. The change in temperature resulting from changes in beam current produced a change in $\int f(p_d)dt$ but in all cases equation 4 was found to hold to better than 5% and in many

cases to better than 2%. This is fairly conclusive evidence that all hydrogen is thermally desorbed and that $\eta < .05$ at equilibrium.

There are three possible processes which might lead to an erroneous result in experiments of this type.

(a) The re-emitted ions and neutrals could have sufficient energy to bury themselves in the walls surrounding the target in which case they would not contribute to the pressure rise in the system. However if this were happening it would simply reduce $\int f(p_b)dt$ and hence make the trapping coefficient even closer to zero.

(b) Any gas introduced into the system might be irreversibly adsorbed on the walls thus lowering the pressure rise both during bombardment and during thermal desorption. However it is reasonably certain that the surface lifetime of hydrogen molecules on stainless steel at room temperature is negligible compared with the times being considered and this has been checked by raising the hydrogen pressure for a sufficient time to saturate all internal surfaces if adsorption was taking place. No change of reflection coefficient indicating saturation has been seen.

(c) The re-emitted ions and neutrals could multiply by desorbing hydrogen adsorbed on the surrounding walls. However in the initial deuterium experiments there was no deuterium on the walls and yet the results were the same as for hydrogen. Moreover the hydrogen yield from the clean targets under deuterium bombardment was very small.

4.2 Absolute Trapping Coefficients: Ti, Ta, Zr.

Measurements of η have been made for titanium, tantalum and zirconium again using Method II. These metals are interesting because they have a high solubility for hydrogen but they are known to release it almost completely at temperatures $\sim 1000^\circ\text{C}$. Borovik⁽¹¹⁾ has recently reported high trapping coefficients for 35 keV H_1^+ ions in titanium and tantalum at room temperature. A typical bombardment and thermal desorption curve for titanium bombarded by 30 keV H_1^+ ions is shown in fig. 5. The marked difference in scale between these two curves and the corresponding ones for molybdenum (fig. 3) is to be noted. Prominent desorption peaks normally obtained in thermal desorption (e.g. Kornelson³)

are visible, but no attempt has been made so far to correlate them with specific activation energies.

No appreciable energy dependence was detected but the trapping did appear to be temperature dependent. With the present turntable arrangement precise temperature measurements were not possible, but the variation of trapping coefficient with temperature obtained by the Methods I and II agreed, making it unlikely that the variations obtained were due to any spurious effects. Both results were consistent with the value relative to molybdenum obtained by switching directly from the Mo target to each of the others using the turntable. The proportionality between the results obtained by the two methods in the temperature range 100-300°C is shown in fig. 6 for all four target materials. The relative trapping coefficients were obtained by Method I from measurements of pressure rise/incident ion current, but for the purpose of comparison with the absolute results obtained by Method II they have been normalized to $\eta_{\text{Mo}} = 0$. Very satisfactory agreement is obtained between the independent measurements on Ti, Ta and Zr, and the extrapolated curve through the Ti, Ta and Zr points agrees fairly well with the assumed value of $\eta = 0$ for molybdenum. Careful extrapolation of the Ti, Ta and Zr results in fact leads to a value of $\eta_{\text{Mo}} = -0.11$, i.e. an apparent re-emission coefficient $R = 110\%$. This negative value of η is probably due to errors in measuring the incident ion current on either Mo or Ti, Ta and Zr. Since the target is biased positively to suppress electrons, differences in secondary ion emission between the different targets would alter the trapping coefficient as measured by Method I by the same amount. A 6% secondary ion emission coefficient for hydrogen ions incident on a tantalum target has been reported by Petrov (12).

4.3 Observations of Gas Sputtering

When a molybdenum target is bombarded first with D_1^+ ions and then with H_1^+ ions re-emission of the deuterium buried during the first bombardment is observed. If following this "gas sputtering" thermal desorption is attempted, very small yields are obtained (compare figs. 4 and 7). This procedure is illustrated in fig. 7. It can be shown by integration that the sum of the yields of deuterium obtained during the initial bombardment, during the gas sputtering with hydrogen, and during the subsequent thermal

desorption is all consistent with 100% re-emission of the deuterium when equilibrium has been reached during the initial bombardment.

This same procedure has been attempted with zirconium and titanium bombarded first with deuterium and then with hydrogen. As shown in fig. 8 less than 0.2% of the trapped deuterium was re-emitted when bombarded with hydrogen, but it was all readily desorbed thermally. These results illustrate a marked difference in trapping mechanism between those metals which combine exothermally with hydrogen and those which do not.

4.4 Dependence of η on dose

A typical curve showing the dependence of trapping coefficient on dose for molybdenum obtained using Method I is shown in fig. 9. It is found that the initial shape of this curve is temperature dependent. However because of the difficulty of measuring temperature in the present experimental arrangement it was found difficult to get reproducible results. At high target temperatures an optical pyrometer could be used and values of η obtained at controlled high temperatures are also shown in fig. 9. The trapping coefficient at equilibrium was found to be the same within experimental error as that at low temperature. Results are also shown for titanium, tantalum and zirconium at low and high temperatures. At low temperature the results are very different from molybdenum, there being a uniformly high trapping coefficient at doses up to at least 5×10^{18} ions/cm². At high temperature however the trapping was very close to molybdenum i.e. $\eta = 0$.

In an attempt to find out the maximum concentration of hydrogen that titanium would absorb before the eventual change to zero trapping coefficient, an attempt was made to presaturate some standard titanium specimens by heating them in a hydrogen atmosphere at 400°C. The change in weight indicated a composition TiH_{0.7}. These samples were then bombarded with H₁⁺ and the trapping coefficient was found to be very similar to a clean titanium metal target except for a large burst of hydrogen gas which was emitted when the target was first bombarded. This was thought to be due to hydrogen adsorbed on the target surface from the residual gas in the vacuum system, which in this case could not be thermally desorbed before bombardment without risk of decomposing

the hydrides. This explanation was confirmed by bombarding with H_1^+ a similarly prepared target which had been "deuterated" rather than "hydrogenated". A trapping coefficient of 0.91 for the incident hydrogen ions was obtained and the initial burst of hydrogen rather than deuterium was observed. No deuterium at all was observed under bombardment until the temperature of the target was raised sufficiently to drive it off thermally. This is illustrated in fig. 10 where the energy of the ion beam was arranged to slowly heat the target up to the critical temperature. Initially the trapping coefficient for the incident beam is high and no deuterium is observed. As the target heats up under the bombardment, the deuterium is evolved at an ever increasing rate. It is noticed that the trapping coefficient of the incident ions is beginning to decrease at the same time. This must be because of the temperature increase rather than saturation as it is not observed when using lower power inputs to the target.

4.5 Energy Dependence of η

Measurements have been made of the trapping coefficient as a function of energy for molybdenum, titanium, tantalum and zirconium (fig. 11). The measurements were taken using Method I at $\sim 100^\circ C$ and under the conditions where the trapping coefficient had reached equilibrium, i.e. at doses $> 10^{17}$ ions/cm². The measurements have been normalized to $\eta = 0$ at 30 keV for molybdenum. Each point is the average of approximately 10 runs. The energy range has been extended to values below 10 keV using H_2^+ and H_3^+ ions and assuming that these are equivalent to 2 or 3 ions with proportionally lower energy. This appears to be justified since the values of η obtained from H_1^+ , H_2^+ and H_3^+ bombardment at 10 keV/atom agree within experimental error.

It is seen that there is no appreciable variation of η with energy in the range 10-30 keV. Below 10 keV the trapping coefficient for Mo appears to decrease slightly relative to that at higher energies. This indicates a steady state re-emission of about 110% of the incident beam which is physically unreasonable. It has been observed repeatedly despite rigorous outgassing. Since these measurements were made by Method I the error is possibly due to a variation with energy of the proportion of ions re-emitted in the charged state, thus affecting relative measurements of beam current.

5. DISCUSSION

5.1 The Method II which has been adopted, because of its elimination of the need for pressure or current calibration, would seem to be the most satisfactory way of obtaining absolute trapping coefficients. The result of $\eta \approx .01$ which has been obtained for Mo is consistent with all the other experimental evidence. A summary of the facts which point to this conclusion is:

(a) Thermal desorption of hydrogen and deuterium from a bombarded Mo target corresponds to that trapped at doses up to 10^{17} ions/cm². For larger doses of up to nearly 10^{20} ions/cm² there is no further increase in the number of ions which can be thermally desorbed.

(b) The equilibrium value of η is independent of energy in the range 10-30 keV.

(c) The equilibrium value of η is independent of temperature in the range 20-900°C.

(d) The values of η for molybdenum deduced from absolute measurements of η in titanium, tantalum and zirconium are each independently consistent with $\eta_{\text{Mo}} = 0$.

(e) The values of η for Ti, Ta and Zr all fall to that of molybdenum at high temperatures.

5.2 The present results shed some light on the mechanism of release of buried atoms. The release rate and the total dose at which saturation takes place for molybdenum, cannot be accounted for in terms of erosion of the metal surface by sputtering, as has been proposed by Burt et al⁽¹³⁾ for heavier ions. The H_1^+ sputtering coefficient of 0.1 for molybdenum⁽¹⁴⁾ is much too low. An alternative explanation in terms of a bombardment induced release mechanism is suggested by the gas sputtering results obtained with molybdenum. These results are similar to the bombardment induced emission of gas from glass surfaces observed by James et al⁽¹⁵⁾. An explanation in terms of gas sputtering must also account for the non release of gas when similar experiments are carried out on reactive metals such as zirconium.

The high trapping coefficients of the reactive metals and the difference in the total quantity of gas released in the reactive and non reactive metals can in fact be explained in terms of

thermal diffusion of the gas in the metal when account is also taken of the barrier potential at the metal surfaces. The incident ions have an initial mean range of several thousand angstroms⁽¹⁶⁾. As bombardment continues their range decreases due to scattering of the incident ions by those already trapped (this has been observed in the case of rare gases⁽⁵⁾), so that a high concentration of hydrogen will tend to build up between the surface and the depth corresponding to the initial range in the solid. The build-up will continue until the rate of loss of hydrogen by escape from the surface and thermal diffusion into the body equals the rate of arrival.

Let us now consider the build up of equilibrium distribution under two extreme conditions. If on the one hand there were no diffusion into the bulk of the metal then equilibrium would be reached when the number of ions back scattered and the number of ions dislodged by incident ions equalled the number arriving. If on the other hand we assume that we have a surface barrier preventing any escape of ions from the surface but a high diffusion rate for the trapped hydrogen in the metal lattice, then the initial distribution will gradually spread through the metal lattice. The distribution can be readily calculated if we assume a δ function source Q , at the plane $x = 0$ of a semi-infinite slab. The solution of the diffusion equation

$$\frac{\partial C}{\partial t} = D \frac{\partial^2 C}{\partial x^2} \quad \dots \quad (5)$$

can be shown to be⁽¹⁷⁾

$$C(x, t) = \frac{Q}{\sqrt{\pi Dt}} \exp\left(\frac{-x^2}{4Dt}\right) \quad \dots \quad (6)$$

The variation of concentration C across a sample of dimensions typical of those used in the present experiment is shown in fig. 12 for various values of Dt . Taking a typical value $t = 1000$ secs it is seen that a diffusion coefficient $D = 10^{-5}$ cm²/sec results in the original distribution of gas being well spread through the bulk of the metal.

In any practical material both re-emission from the surface and diffusion into the bulk must be taking place simultaneously. There are however, two major differences between the hydrogen reactive metals and the non hydrogen-active ones which can explain

the difference in behaviour of their respective trapping coefficients. The first is simply that the exothermic reaction implies a potential barrier at the surface for any hydrogen atom in the metal. The size of the barrier depends to some extent on the concentration of hydrogen in the metal, but results obtained from heat of solution experiments shown in Table I indicate values in the region 20-40 k.cals/mole.

The second difference between the two classes of metals is that in general the diffusion coefficients are higher in the reactive ones than in the unreactive ones and that the activation energy for diffusion is lower. The lower activation energies are only apparent when measurements of the diffusion coefficients in the reactive metals are made by a technique which involves transport solely within the metal rather than across the surface, where the heat of the solution may predominate. Unfortunately very few measurements have been made in this way but those which are available are quoted in Table II, the diffusion coefficient being expressed in the usual form $D = D_0 \exp\left(\frac{-E}{RT}\right)$.

The values quoted in Tables I and II show that for titanium, zirconium and niobium the activation energy for diffusion is considerably smaller than the heat of solution. The differences in behaviour between the endothermic non reactive metals and the exothermic reactive metals is most easily visualized by means of an energy diagram, fig. 13.

It is now clear why the reactive metals have high trapping coefficients. The potential barrier at the surface prevents the escape of migrating atoms and the diffusion coefficient allows the atoms to diffuse into the bulk of the metal, which with its high solubility provides an effectively infinite reservoir for the beam currents which have been used. The small fraction of the incident particles which is not trapped may be due to those ions which are deflected through 180° by a small number of large angle scattering collisions in the lattice and arrive back at the surface with sufficient energy to escape.

For the non reactive metals as soon as the initial concentration begins to rise at the mean ion range, if there is no potential barrier at the surface the surface concentration will be zero and there will be a steep concentration gradient towards the

surface. At equilibrium the concentration gradient from the mean ion range away from the bombarded surface must be so small that the main diffusion flow of the trapped ions is towards the bombarded surface as illustrated in fig. 14. This will be the case where the target thickness is much greater than the range of the incident ions.

The model described will also explain the results obtained during the gas sputtering experiments. Here it was found that on bombarding a Mo target initially with D_1^+ ions and then with H_1^+ that nearly all the D_1^+ ions trapped during the first bombardment were released on bombardment with H_1^+ ions. Similar observations where a large fraction, though not always 100% of the trapped ions are re-emitted have been made on other non reactive metals. However in the case of Zr and Ti only a very small fraction of the trapped ions could be released when the same experiment was attempted. If we consider again the concentration distribution of the gas in the metal predicted by equation (6) then we can calculate the total quantity Q^1 of gas within the layer between the surface and the range of incident ions R

$$Q^1 = \int_0^R C(x,t) dx$$

$$= \frac{Q}{\sqrt{\pi Dt}} \int_0^R \exp \frac{-x^2}{4Dt} dx \quad \dots (7)$$

i.e. the number of buried ions with the range R is uniquely determined by Dt.

Taking a range $R = 2 \times 10^{-5}$ cms as typical of 20 keV H_1^+ ions in metals⁽¹⁶⁾ we obtain on integrating (7)

For Dt = 10^{-4}	$Q^1/Q = 0.1\%$
Dt = 10^{-6}	$Q^1/Q = 1.1\%$
Dt = 10^{-8}	$Q^1/Q = 11\%$
Dt = 10^{-9}	$Q^1/Q = 35\%$
Dt = 10^{-10}	$Q^1/Q = 88\%$

Assuming that all those ions which are within range R can be dislodged by further bombardment then the fraction re-emitted is a measure of the diffusion coefficient. This calculation is not however likely to be quantitative until a more realistic approximation than the δ function is used for the form of the initial ion distribution and the mean ion range. On the basis of the present calculation the difference between the high gas sputtering yield

for Mo and the low yield from Zr could be explained by a difference of $\sim 10^4$ in their respective diffusion coefficients, which is larger than the difference in the reported values. Further investigation of the measurements of the diffusion coefficients are desirable. There is still however the possibility that the small percentage of buried ions which are gas sputtered from Ti and Zr is due to the high potential barrier of the surface rather than to the high diffusion coefficient keeping the concentration low near the surface. The importance of the surface barrier could be determined by investigating the gas sputtering over a large temperature range since the diffusion coefficient will vary exponentially with temperature and thus vary the concentration within the range of the incident ions. Although no systematic data is available, Borovik⁽¹¹⁾ has shown that the trapping coefficient for Ti decreases with dose at 100°K and thus it seems that the diffusion process plays the dominant role.

6. CONCLUSION

The use of the technique of partial pressure rise measurements during bombardment and during subsequent thermal desorption of trapped ions has been found to be a convenient and reliable method of measuring the absolute trapping coefficient of ions in metals. The behaviour for molybdenum when compared with results for tungsten and stainless steel already reported⁽¹⁰⁾, would seem to indicate that it is typical of metals which do not react exothermically with hydrogen. This has been confirmed by more recent results on Al, Cu, Fe, Ni and Pt.

The measurements made with hydrogen ions on Ti, Ta, and Zr show that it is possible to obtain trapping coefficients $\eta > 0.9$ at or near room temperature. This high trapping coefficient may be of considerable practical importance in the design of certain types of nuclear fusion research experiments.

The results of the trapping coefficient measurements and of the experiments on gas sputtering have been explained in terms of a model which takes into account the diffusion rate and the heat of the solution of the gas in the metal.

ACKNOWLEDGEMENTS

The authors are grateful to H. H. H. Watson for many valuable discussions in the course of this work.

TABLE I

SOLUBILITY OF HYDROGEN AND DEUTERIUM IN METALS

System	Concentration Range Atomic Ratio	Heat of Solution kcal/mole ΔH	Ref.
Ti-H ₂	<0.1	21.6	18
Ti-H ₂	< .04	19	19
	0.21-1.3	27-34	
Zr-H ₂	< .02	29	19
	0.69-1.15	33-40	
Zr-H ₂	.025-1.74	34.9	20
Ti-D ₂	.02-0.1	22.5	21
	0.2-1.8	31.8-29.1	
Zr-D ₂	.02-.05	29	21
	0.2-1.8	38.9-32.9	
Nb-H ₂	.01-0.1	15.9-16.9	22
	0.2-0.7	18.1-23.0	
Pd-H ₂	?	2.04	23
Mo-H ₂	-	- 3.5	23
Cu-H ₂	-	- 14.1	23
Ni-H ₂	-	- 5.6	23

TABLE II

DIFFUSION OF HYDROGEN IN METALS

Metal	Diff. Coeff. at 100°C cm ² /sec	D ₀ cm ² /sec	E kcal/mole	Ref.
Molybdenum	8.5 x 10 ⁻¹⁰	7.6 x 10 ⁻⁵	8.4	24
Austenitic S/S EN58E	7.1 x 10 ⁻¹⁰	2.1 x 10 ⁻³	11.0 15.6	24 25
Ferritic S/S	2 x 10 ⁻⁶		6.5	25
Copper	9.3 x 10 ⁻¹⁰	1.6 x 10 ⁻⁵	7.2	24
Nickel	1.6 x 10 ⁻⁸	2.04 x 10 ⁻³	8.7	26
Zirconium	10 ⁻⁷		7.06 5.7	27 28
Niobium			3.7-5.0	29
Tantalum			2.6-3.7	30
Palladium	1.5 x 10 ⁻⁶		6.8	31
Titanium	-		5.3 9.4-10.2	32 33

REFERENCES

1. VARNERIN, L.J. and CARMICHAEL, J.H. J. Appl. Phys. 28, 913, 1957.
2. COLLIGON, J.S. and LECK, J.H. Trans. 8th A.V.S. Nat. Vac. Symp. 275, 1961.
3. KORNELSON, E.V. Can. J. Phys. 42, 364, 1964.
4. ALMEN, O. and BRUCE, G. Nucl. Instr. and Methods 11, 257, 1961.
5. BROWN, F. and DAVIES, J.A. Can. J. Phys. 41, 844, 1963.
6. GRANT, W.A. and CARTER, G. Vacuum 15, 477, 1965.
7. SIMONOV, V.A., KLEIMONOV, G.F., MILESHKIN, A.G. and KOCHNEV, K.A. Nuclear Fusion 1, 325, 1962.
8. BOROVNIK, E.S., KATRICH, N.P. and NIKOLAEV, G.T. Atomnaya Energiya 18, 91, 1965.
9. McCRACKEN, G.M., MAPLE, J.H.C. and WATSON H.H.H. Rev. Sci. Inst. 37, 860, 1966.
10. McCRACKEN, G.M. and MAPLE, J.H.C. VIIth Int. Conf. on Ionization Phenomena in Gases, Belgrade, Aug. 1965 (to be published in 1966).
11. BOROVNIK, E.S., KATRICH, N.P. and NIKOLAEV, G.T. VIIth Int. Conf. on Ionization Phenomena in Gases, Belgrade, Aug. 1965 (to be published in 1966).
12. PETROV, N.N. Sov. Phys. Solid State 2, 857, 1960.
13. BURTT, R.B., COLLIGON, J.S. and LECK, J.H. Brit. J. Appl. Phys. 12, 396, 1961.
14. WEHNER, G.K., KENKNIGHT, C. and ROSENBERG, D.L. Planet Space Science 11, 885, 1963.
15. JAMES, L.H., LECK, J.H. and CARTER, G. Brit. J. of Appl. Phys. 15, 681, 1964.
16. YOUNG, J.R. J. Appl. Phys. 27, 1, 1956.
17. BARRER, R.M. "Diffusion in and through solids" p.45, C.U.P., 1951, 2nd Ed.
18. McQUILLAN, A.D. Proc. Roy. Soc. 104, 309, 1950.
19. SOF'INA, V.V. and PAVLOVSKAYA, N.G. Russ. J. of Phys. Chem. 34, 525, 1960.
20. GULBRANSON, E.A. and ANDREW, K.F. J. Electrochem. Soc. 101, 474, 1954.
21. MORTON, J.R. and STARK, D.S. Services Electronics Research Laboratory Technical Journal 10, 12, 1960.
22. ALBRECHT, W.M., GOODE, W.D. and MALLET, M.W. Report No. B.M.I. 1332, Battelle Memorial Inst. Columbus, Ohio, 1959.
23. BARRER, R.M. op. cit. pg. 153.
24. JONES, P.M.S., GIBSON, R. and EVANS, J.A. Report No. A.W.R.E. 0-16/66. Atomic Weapons Research Establishment, Aldermaston, Berks. 1966.
25. ESHBACH, H.L., GROSS, F. and SCHULIEN, S. Vacuum 12, 543, 1963.

26. BARRER, R.M. op. cit. pg. 222.
27. MALLETT, M.W. and ALBRECHT, W.M. J. Electrochem Soc. 104, 142, 1957.
28. SAWATZKY, A. J. of Nucl. Mat. 9, 364, 1963.
29. ZAMIR, D. and COTTS, R.M. Phys. Rev. 134, A670, 1964.
30. PEDERSON, D., KROGDAHL, T. and STOKKELAND, O.E. J. Chem. Phys. 42, 72, 1965.
31. BARRER, R.M. op. cit. pg. 221.
32. MARSHALL, R.P. Trans. Met. Soc. A.I.M.E. 233, 1449, 1965.
33. STALINSKI, B., COOGAN, C.K. and GUTOWKSY, H.S. J. Chem. Phys. 34, 1191, 1961.

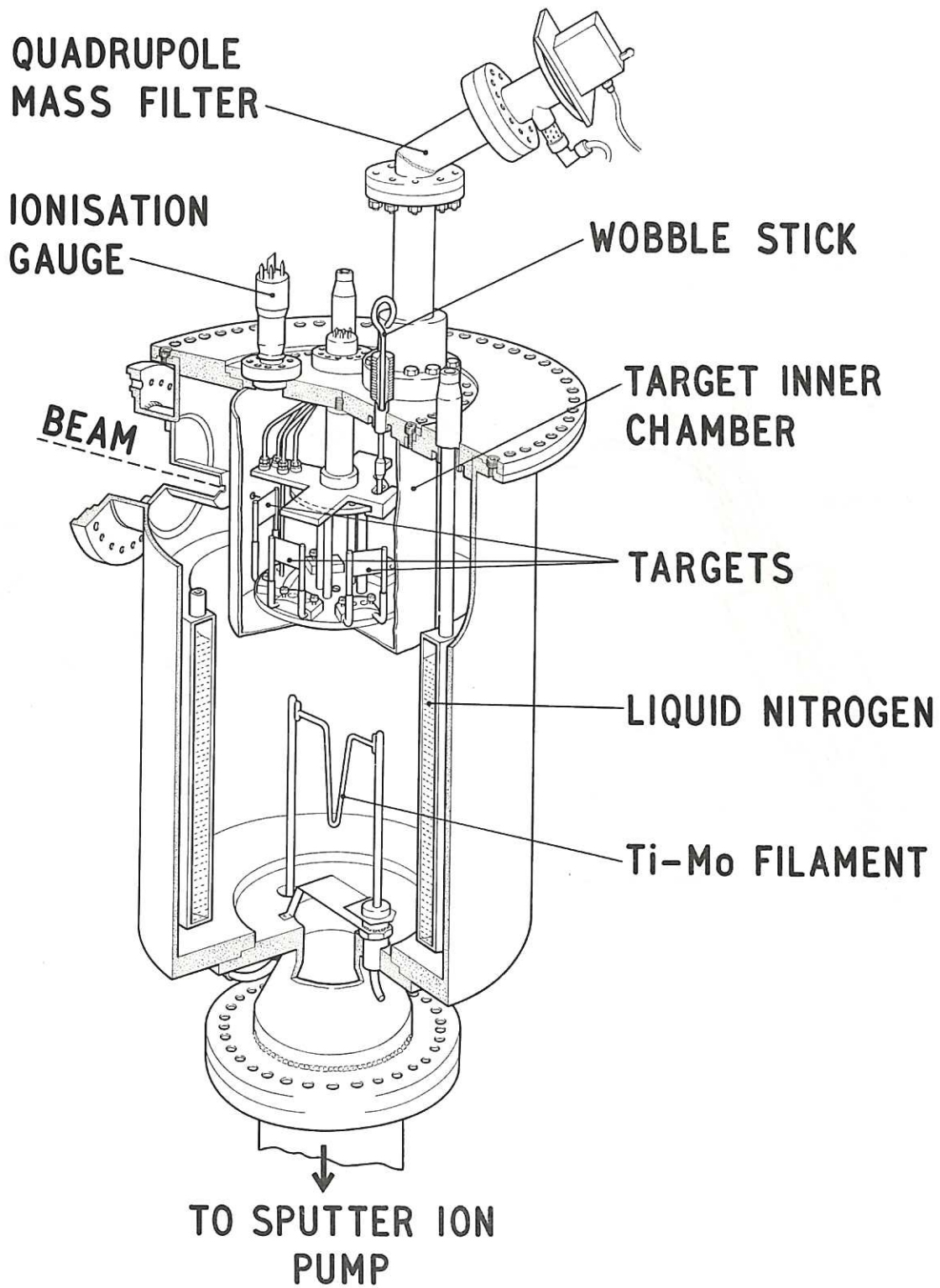


Fig. 1 Schematic diagram of ion bombardment apparatus (CLM-P 118)

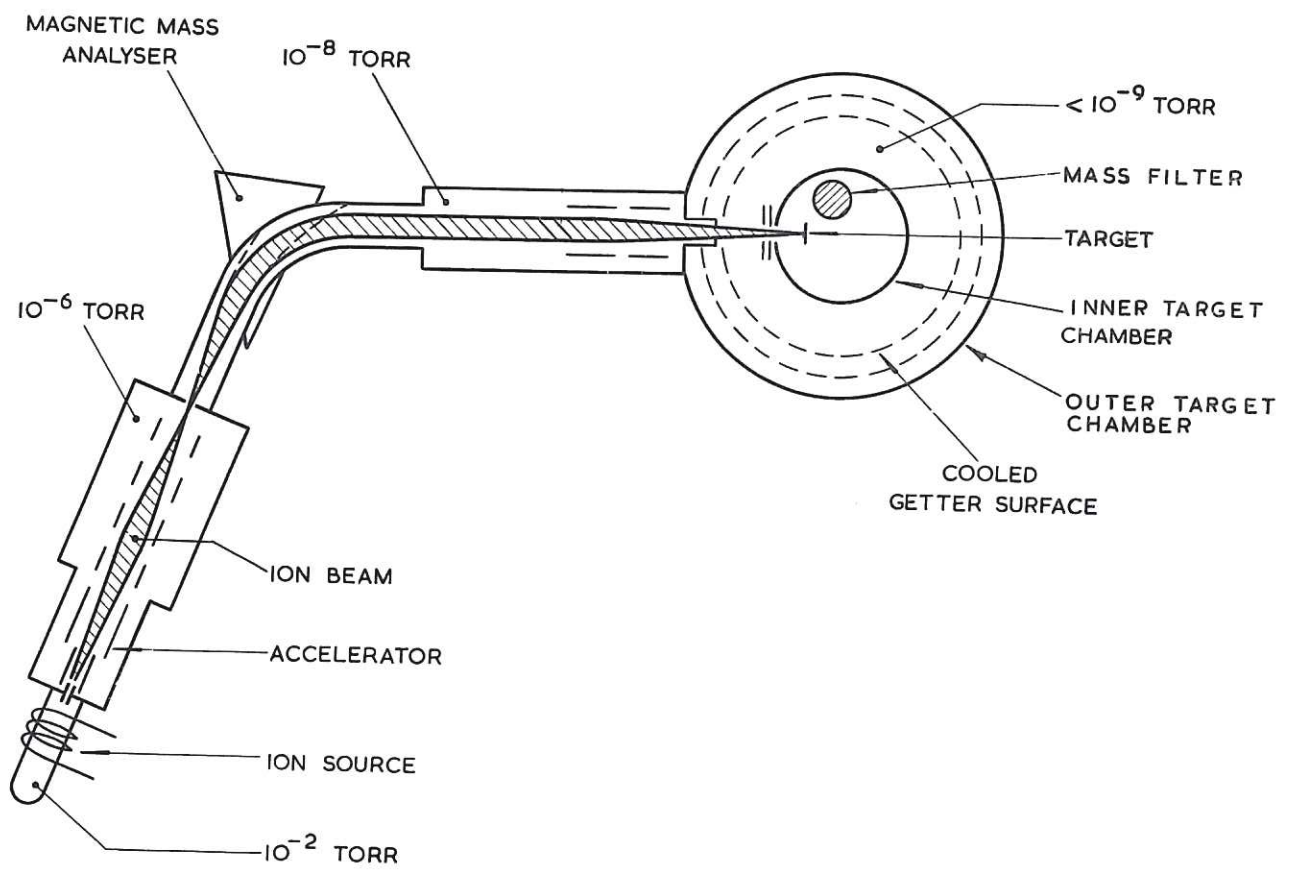


Fig. 2 Details of target chamber (CLM-P118)

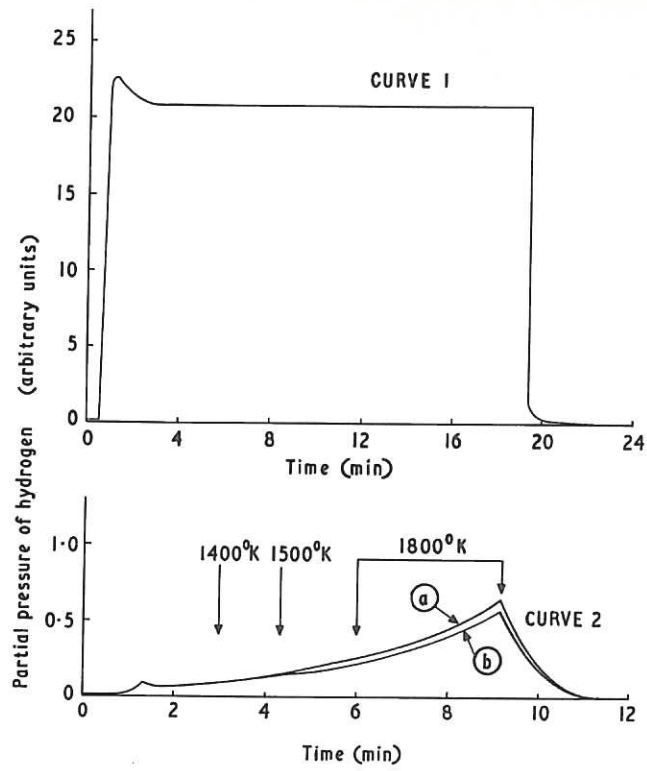


Fig. 3 (CLM - P 118)
 Curve 1. Molybdenum target bombarded with $95 \mu\text{A}$, 30 keV , H_1^+ ions. Curve 2. Thermal desorption of molybdenum, (a) Following above run; (b) On clean target

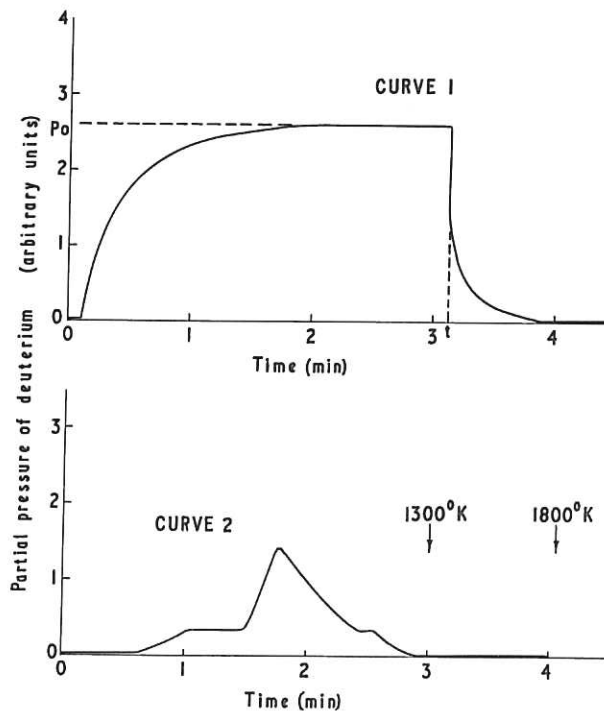


Fig. 4 (CLM - P 118)
 Curve 1. Molybdenum target bombarded with $18 \mu\text{A}$, 20 keV , D_1^+ ions. Curve 2. Thermal desorption of deuterium from molybdenum following above run

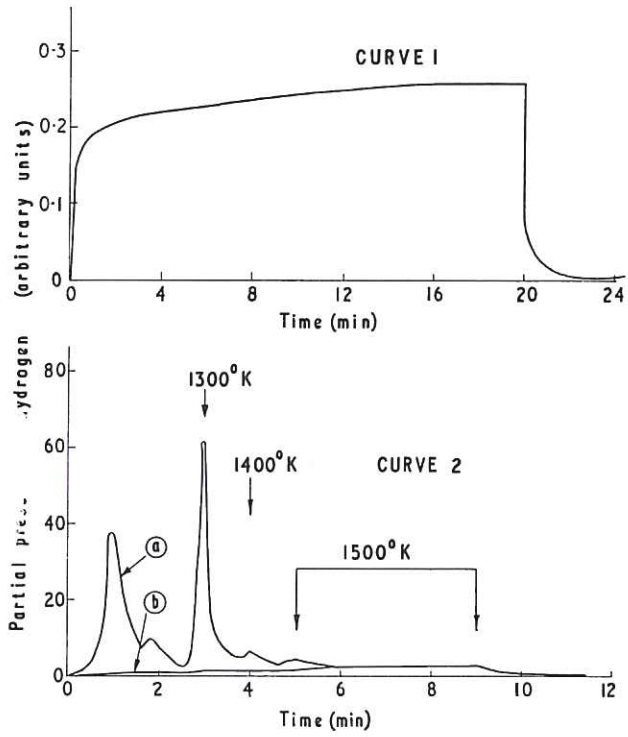


Fig. 5 (CLM-P 118)
 Curve 1. Titanium target bombarded with $12 \mu\text{A}$, 30 keV , H^+ ions. Curve 2. Thermal desorption of hydrogen from titanium - (a) Following above run; (b) On clean target

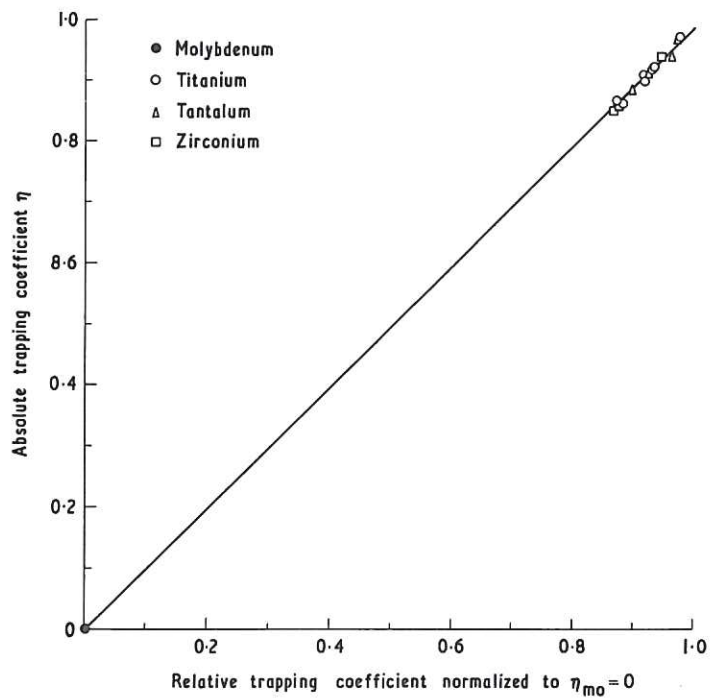


Fig. 6 (CLM-P 118)
 Comparison of Methods I and II for measuring trapping coefficients

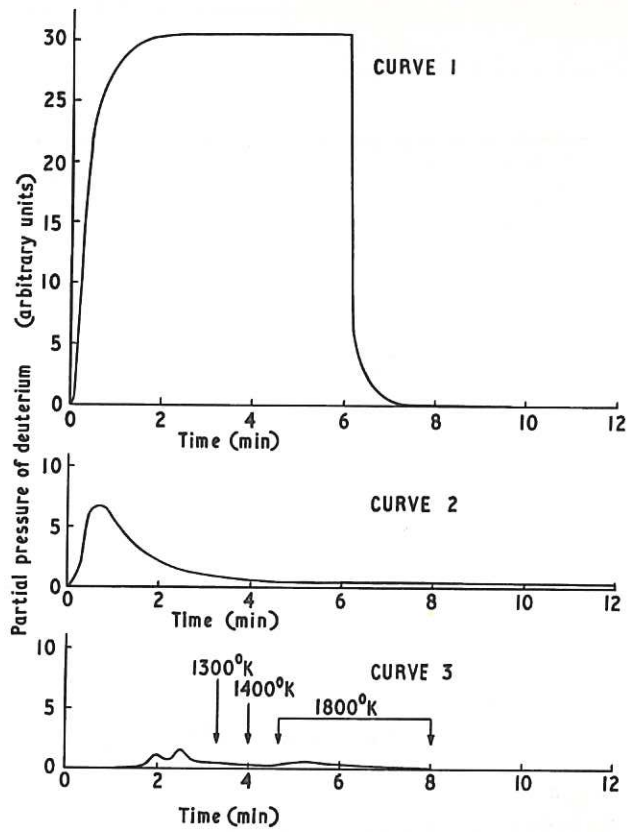


Fig. 7 (CLM-P 118)

Gas sputtering on molybdenum target
 Curve 1. Bombardment with $18 \mu\text{A}$, 20 keV, D_1^+ ions
 Curve 2. Gas sputtering by $18 \mu\text{A}$, 20 keV, H_1^+ ions
 Curve 3. Thermal desorption following previous run

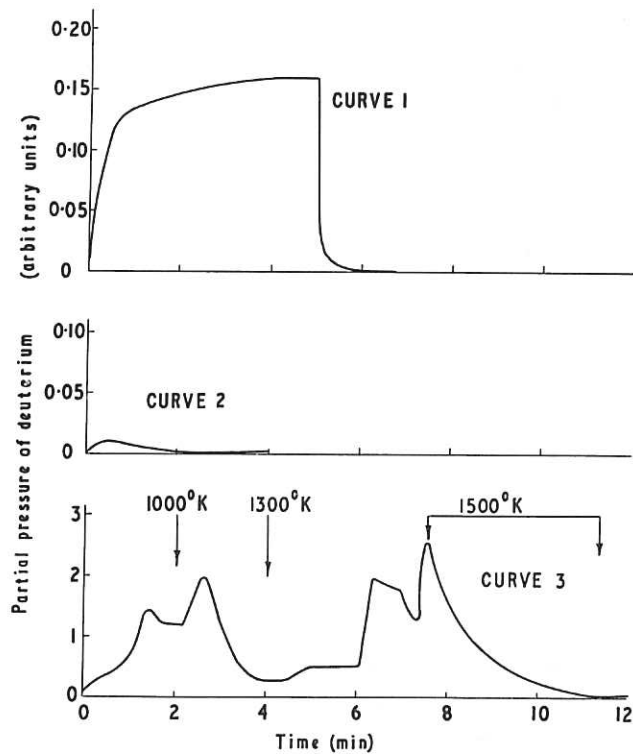


Fig. 8 (CLM-P 118)

Gas sputtering on zirconium target
 Curve 1. Bombardment with $12 \mu\text{A}$, 20 keV, D_1^+ ions
 Curve 2. Gas sputtering by $12 \mu\text{A}$, 20 keV, H_1^+ ions
 Curve 3. Thermal desorption following previous run

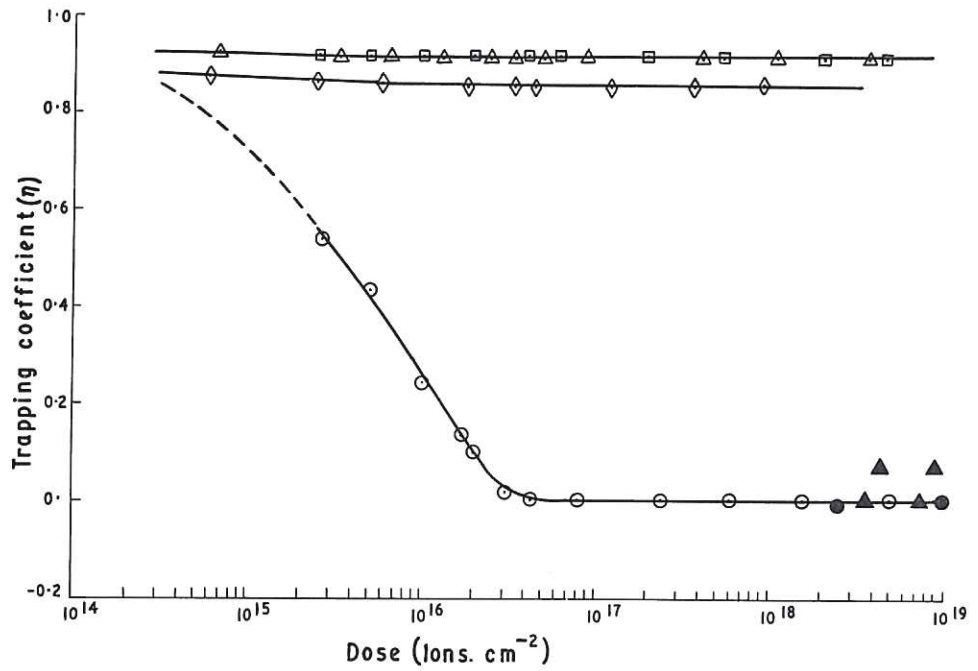


Fig. 9 (CLM-P118)
 Variation of trapping coefficient of H_1^+ ions with dose

\circ Mo $\sim 100^\circ\text{C}$ 10 keV	\triangle Ti $\sim 100^\circ\text{C}$ 10 keV
\bullet Mo $\sim 900^\circ\text{C}$ 30 keV	\square Zr $\sim 100^\circ\text{C}$ 10 keV
\blacktriangle Ti $\sim 900^\circ\text{C}$ 30 keV	\diamond Ta $\sim 100^\circ\text{C}$ 10 keV

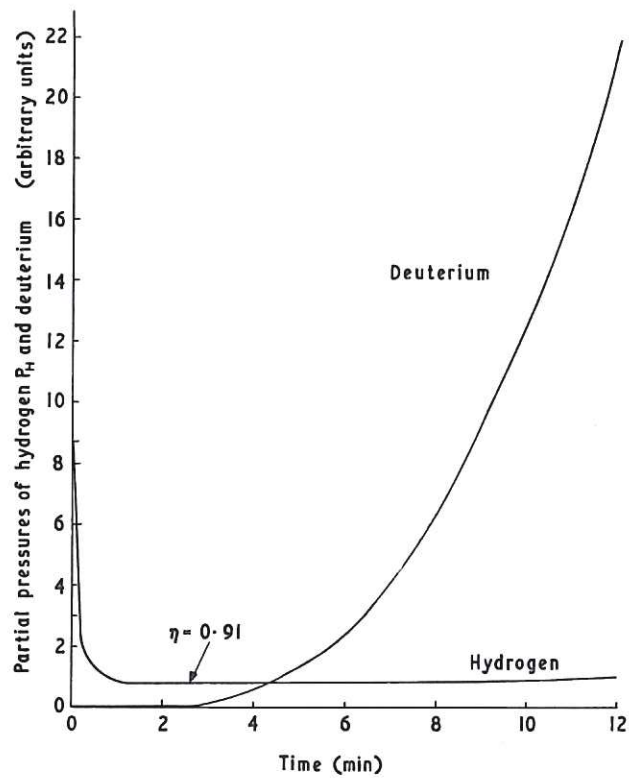


Fig. 10 (CLM-P118)
 Deuterated titanium target, composition $\text{TiH}_{0.7}$
 bombarded with $38 \mu\text{A}$ H_1^+ ions

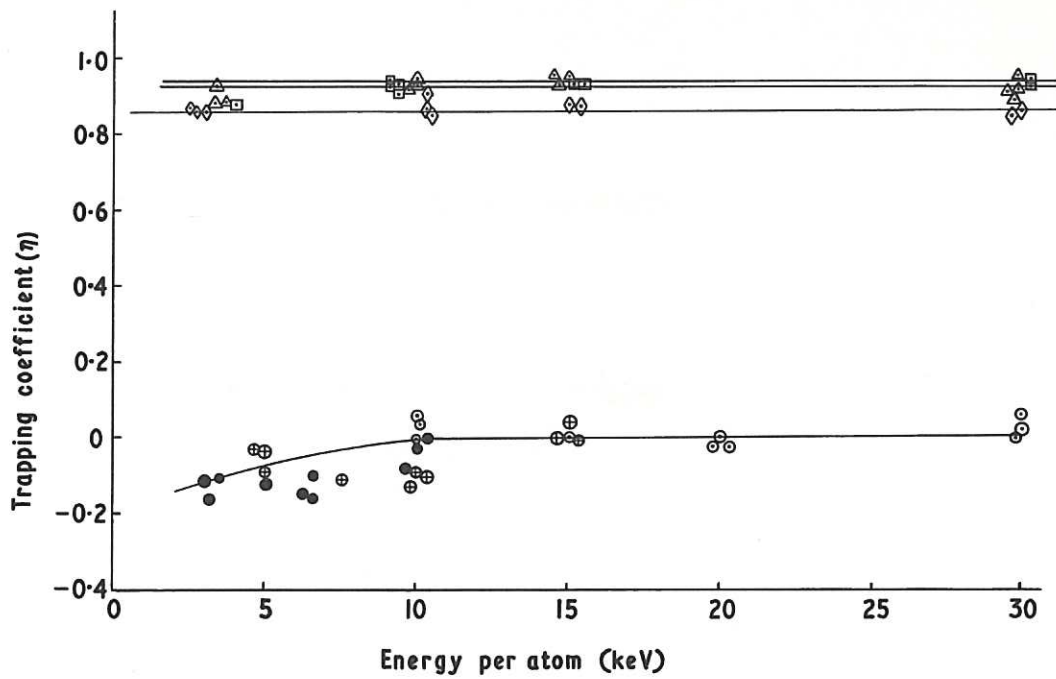


Fig. 11 (CLM-P 118)
Variation of trapping coefficient of hydrogen ions with energy.

Dose $> 10^{17}$ ions/cm²

○ Mo	H_1^+	△ Ti
⊕ Mo	H_2^+	□ Zr
● Mo	H_3^+	◇ Ta

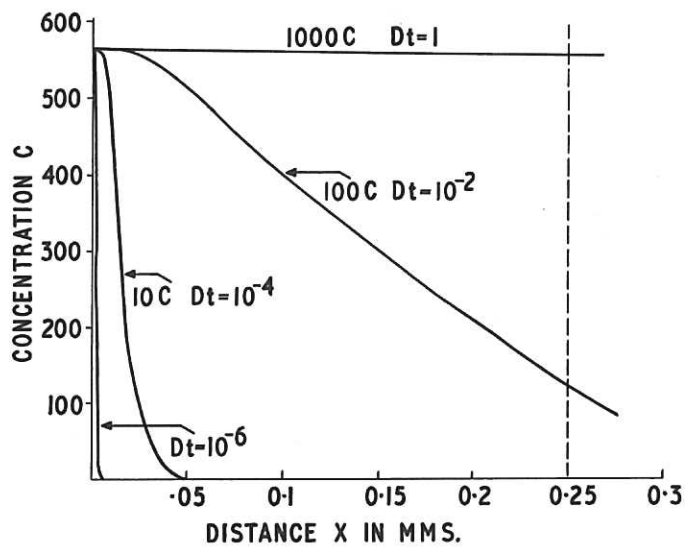


Fig. 12 (CLM-P 118)
Distribution of a solute in a semi-infinite slab for various values of Dt where D is the diffusion coefficient in cm²/sec and t is the time in seconds

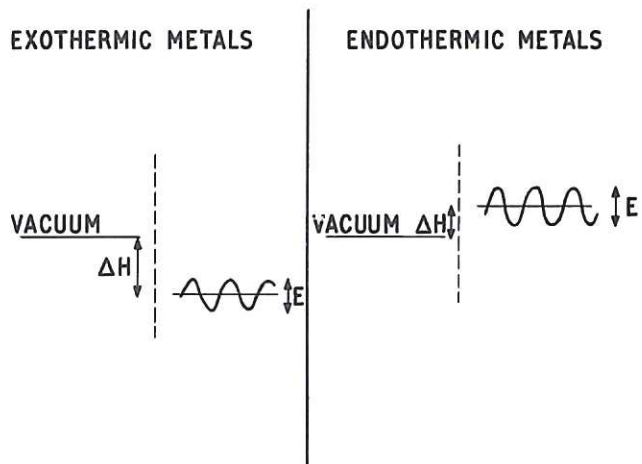


Fig. 13 (CLM-P 118)
 Schematic diagram of the energy levels of hydrogen atoms in endothermic and exothermic metals. ΔH represents the heat of solution of the gas in the metal, and E the activation energy for diffusion

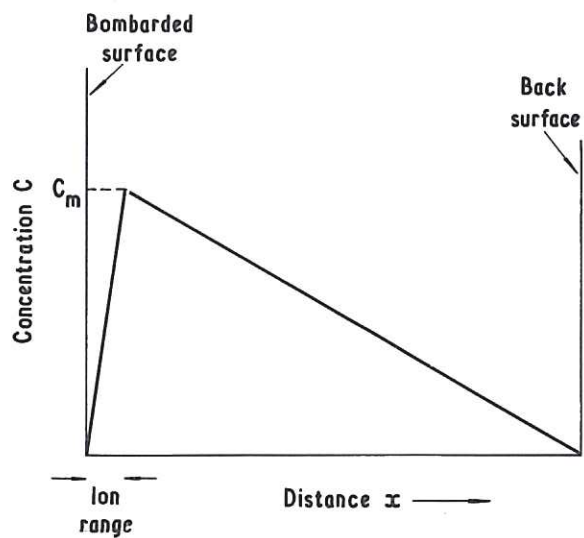
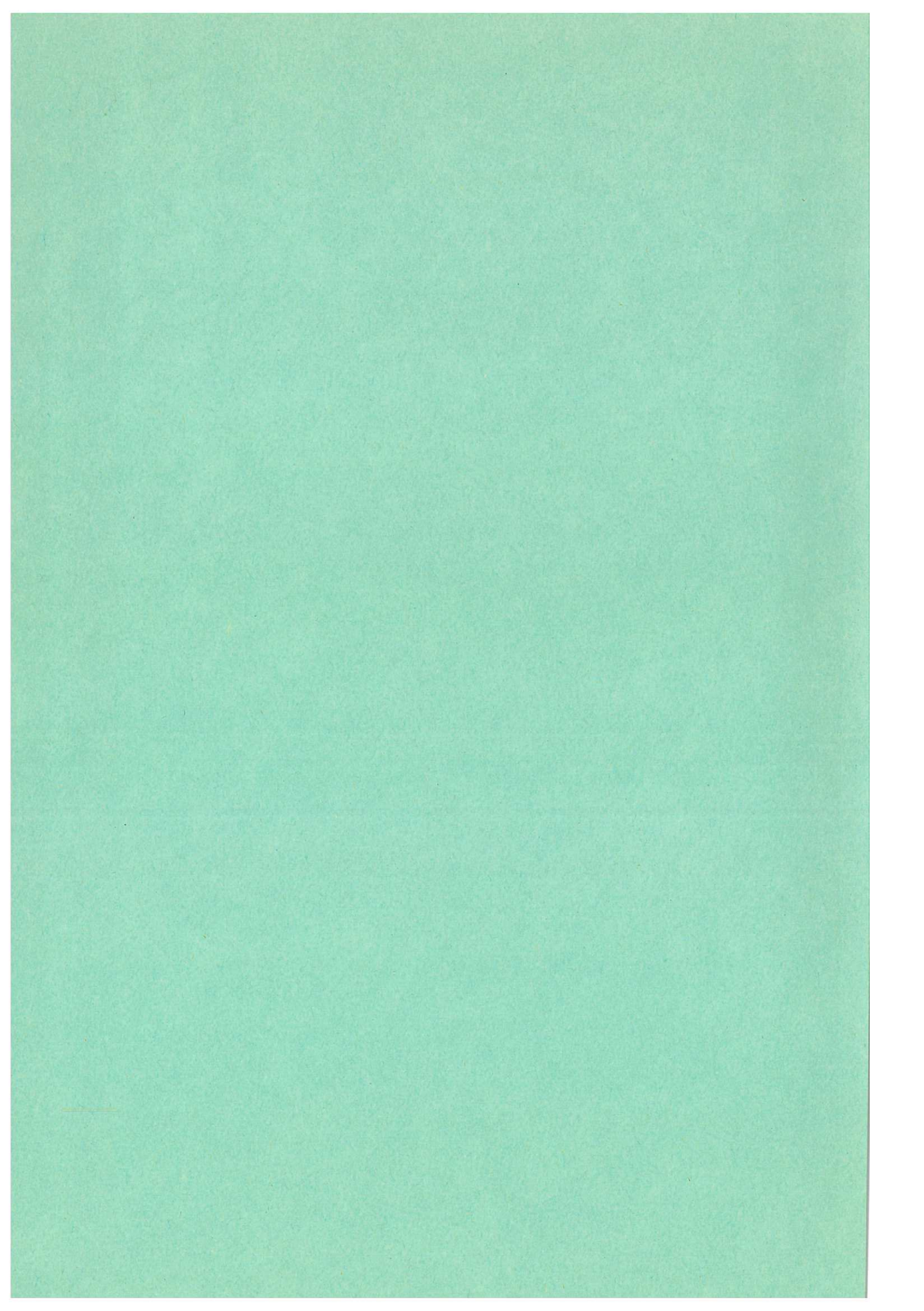


Fig. 14 (CLM-P 118)
 Concentration distribution of gas in metal target under steady state ion bombardment, assuming surface concentration is zero



100
101
102
103
104
105
106
107
108
109
110
111
112
113
114
115
116
117
118
119
120
121
122
123
124
125
126
127
128
129
130
131
132
133
134
135
136
137
138
139
140
141
142
143
144
145
146
147
148
149
150
151
152
153
154
155
156
157
158
159
160
161
162
163
164
165
166
167
168
169
170
171
172
173
174
175
176
177
178
179
180
181
182
183
184
185
186
187
188
189
190
191
192
193
194
195
196
197
198
199
200